Journal of Ceramic Processing Research. Vol. 23, No. 2, pp. 149~153 (2022)
(Received 18 May 2021, Received in revised form 5 October 2021, Accepted 9 October 2021)
https://doi.org/10.36410/jcpr.2022.23.2.149

J O U R N A L O F
Ceramic Processing Research

Effect of $MgO-CaO-Al_2O_3-SiO_2$ glass additive on densification of Al_2O_3 ceramics

Dagyeong Lee[a,b], Hyun Seon Hong[b], Hyeondeok Jeong[a,*] and Sung-Soo Ryu[a,*]
[a]*Engineering Ceramic Center, Korea Institute of Ceramic Engineering and Technology, Icheon 17303, Republic of Korea*
[b]*Department of Environment & Energy Engineering, Sungshin Women's University, Seoul 01133, Republic of Korea*

We investigated the effect of the $MgO-CaO-Al_2O_3-SiO_2$ (MCAS) additive on the densification of Al_2O_3 ceramics. MCAS was synthesized using a polymeric-complex method. We analyzed the densification behavior, using dilatometric analysis up to 1600 °C, and the results showed that sinterability increased with increasing MCAS content. Al_2O_3 samples were prepared by isothermal sintering at 1400, 1500, and 1600 °C. The microstructure, phase formation, and hardness of the samples were analyzed and discussed in relation to both the MCAS content and sintering temperature. The density of the MCAS-doped samples sintered at 1500 and 1600 °C was over 98%, and the maximum relative density was 99.7%. The highest hardness (18 GPa) was achieved for the sample prepared with 3 wt.% MCAS and sintered at 1500 °C for 1 h because further doping resulted in excessive grain growth. These results elucidate the conditions required for pressure-free sintering.

Keywords: Al_2O_3, Sintering additive, MCAS glass, Dilatometry, Densification.

Introduction

Alumina (Al_2O_3) is a ceramic material that exhibits excellent thermal, mechanical, and chemical properties. It is widely used in electronics, heat-resistant equipment, and mobile technologies. Many studies have been conducted on the densification and grain growth of Al_2O_3 materials [1-8]. However, recent technological advances in related industries have increased the demand for Al_2O_3 materials exhibiting enhanced dielectric properties and plasma resistance. Therefore, research on advanced sintering methods and additives for Al_2O_3 materials has been attracting increasing attention [9-14].

Novel sintering methods including isostatic pressing, hot pressing, and gas-pressurized sintering can be employed to densify Al_2O_3 [1-3, 6]. These pressurization-based methods require expensive equipment, involve dangerous processes, and limit the size of the resulting ceramics. Therefore, researchers have used additives to attempt to develop pressure-free sintering methods. Several studies have used sintering aids such as NiO, SiO_2, MnO, FeO, MgO, and TiO_2 to improve sintering density and other properties [10, 15-17]. However, the additives usually degrade the mechanical and/or electrical properties of Al_2O_3 materials.

Glass-ceramic additives such as $MgO-Al_2O_3-SiO_2$ (MAS), $Li_2O-Al_2O_3-SiO_2$ (LAS), $CaO-Al_2O_3-SiO_2$ (CAS), and $MgO-CaO-Al_2O_3-SiO_2$ (MCAS) are polycrystalline materials consisting of fine grains and effectively accelerate sintering and improve the properties of ceramic materials [11-13, 18-22]. Specifically, the addition of MCAS glass can increase the density and enable the control of the microstructure of ceramic materials without significantly altering their properties. Alumina materials prepared using glass-ceramic additives are expected to be applied to spark plugs, ceramic tiles/fibers, electrostatic chucks, and insulators.

C. Cheng et al. studied the addition of MCAS to $BaTi_4O_9$- and $Ba_2Ti_9O_{20}$-based ceramics and reported that the densification temperature of the ceramic materials was lowered with the addition of the MCAS [19]. H. Lee et al. investigated the sintering behavior of AlN ceramics prepared with added MCAS and showed that the addition of 5 wt.% MCAS significantly densified the AlN ceramics [20, 21]. However, few studies have been conducted on the effect of MCAS on the densification properties of Al_2O_3 materials.

Therefore, to investigate sinterability, MCAS was added to Al_2O_3 in varying concentrations in this study. Isothermally sintered Al_2O_3 was also prepared at different temperatures; the density, phase, and microstructure were analyzed; and the relation between the MCAS content and the sintering temperature was investigated.

Experimental Method

Commercial Al_2O_3 (AES-11, Sumitomo Chemical, Japan) and MCAS glass prepared using a polymeric-complex method were used as raw materials [23]. Fig. 1 shows SEM (scanning electron microscopy) images of the Al_2O_3 and MCAS used in this study. The Al_2O_3 (Fig. 1(a)) and MCAS (Fig. 1(b)) exhibited particle sizes of approximately 500 and 50 nm, respectively.

*Corresponding author:
Tel : +82 31 645 1482
Fax: +82 31 645 1485
E-mail: jhd526@kicet.re.kr (H. Jeong), ssryu@kicet.re.kr (S.-S. Ryu)

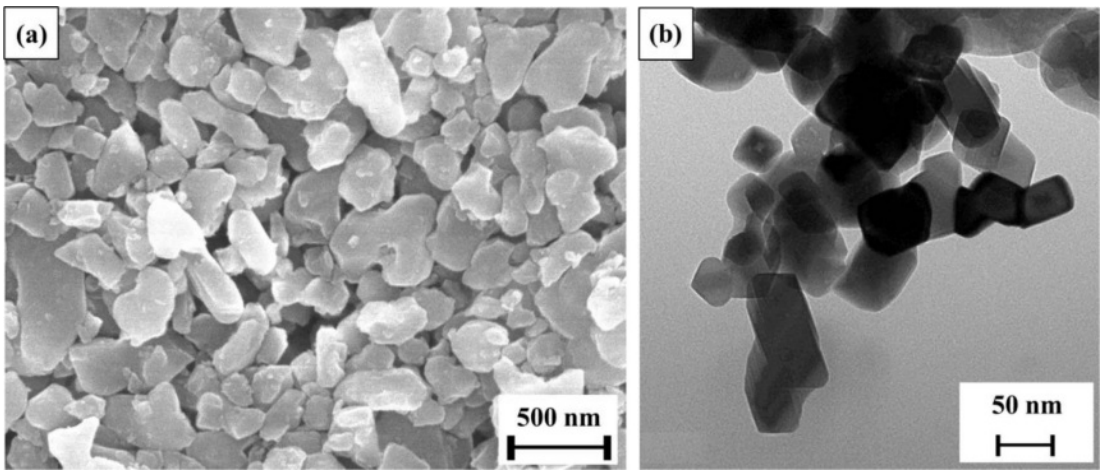

Fig. 1. FE-SEM image of (a) Al_2O_3 powder and (b) MCAS additive used in this study.

The synthesized MCAS (1, 3, or 5 wt.%) was added to Al_2O_3 and mixed using a planetary mill (PULVERISETTE 6, Fritsch, Germany). Subsequently, 20 g of the Al_2O_3-MCAS mixed powder, 0.2 g of dispersant (BYK-111, BYK, Germany), 100 g of Al_2O_3 balls (diameter: 5 mm), and 150 mL of isopropyl alcohol (Merck, Germany) were mixed at 300 rpm for 1 h. The mixture was dried in an oven at 80 ºC for 20 h to evaporate the isopropyl alcohol. The 0, 1, 3, and 5 wt.% MCAS mixed powders were designated as M0, M1, M3, and M5, respectively.

The temperature-dependent sintering behavior was analyzed using a dilatometer (DIL-402C, Netzsch, Germany). The mixed powders were compacted into 12-mm-long cylinders, using a uniaxial press at 150 MPa. The thermal expansion of the pushrod was measured previously with nondoped Al_2O_3 samples. The linear shrinkage was measured while heating the prepared samples at 5 ºC/min to 1600 ºC, where the samples were held for 1 h. To determine the effect of the sintering temperature on the Al_2O_3 properties, additional specimens were heated at 5 ºC/min and sintered at 1400 and 1500 ºC for 1 h.

Sample density was measured using Archimedes' principle. The microstructure was analyzed using a scanning electron microscope (SEM; JSM-6390, JSM-7500F, JEOL, Japan). The crystallinity was analyzed using an X-ray diffractometer (XRD; D/max-2500, RIGAKU, Japan) operating at 40-kV acceleration and 100 mA and with a scanning angle in the range 20-80º and a scanning rate of 10°/min. Sample hardness was measured under a load of 0.5 kg·f, using a Vickers hardness tester (810-165K, Mitutoyo, Japan).

Results and Discussion

Dilatometer analysis

Fig. 2 presents the shrinkage behaviors of M0, M1, M3, and M5. Based on these results, the shrinkage onset and offset temperatures (T_{onset} and T_{offset}, respectively) and the maximum shrinkage temperature (T_{max}), are summarized in Table 1. Fig. 2(a) shows that M0 exhibited a lower T_{onset} (1189 ºC) than the other samples. However, M0 continued to shrink until 1600 ºC, indicating slower densification over a wider temperature range. Additionally, as shown in the shrinkage-rate curves in Fig. 2(b), the maximum shrinkage rate of M0 was approximately 0.2 %/min, which is about half that of the MCAS-containing samples. For M1, M3, and

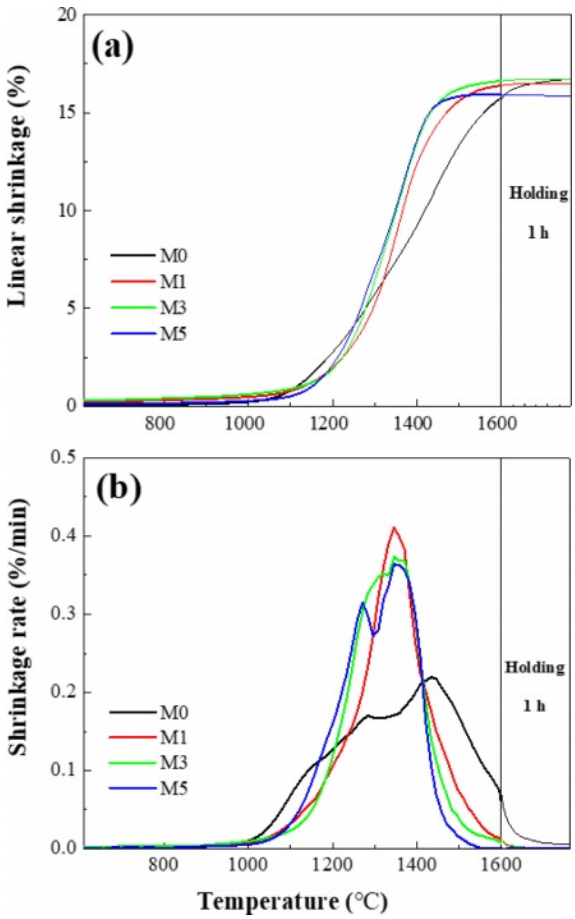

Fig. 2. Dilatometry analysis results for alumina with respect to MCAS content: (a) linear shrinkage and (b) shrinkage rate.

Table 1. Onset and maximum shrinkage temperature based on dilatometry results.

Specimen	T_{onset} (°C)	T_{max} (°C)	T_{offset} (°C)
M0	1189	1445	≥1600
M1	1256	1357	1570
M3	1231	1370	1545
M5	1206	1382	1508

M5, shrinkage started at a relatively high temperature but occurred rapidly over a narrow temperature range. These results are presumably related to the thermal expansion and melting of the MCAS additive. The MCAS used in this study exhibited a higher coefficient of thermal expansion than Al_2O_3. Moreover, MCAS reportedly melts at approximately 1050 °C [24]. Thus, the heating- and melting-induced volumetric expansion appears to have offset the shrinkage caused by Al_2O_3 sintering. However, the MCAS melted and formed a neck between the Al_2O_3 particles and accelerated sintering. M1, M3, and M5 were completely sintered below 1600 °C. In addition, the higher the MCAS content, the lower the value of T_{offset}.

Sintering density

Fig. 3 shows the relative densities measured as per Archimedes' principle for the samples sintered at 1400, 1500, and 1600 °C for 1 h. The relative densities of M0 sintered at 1400 and 1600 °C were 81 and < 95%, respectively. The relative densities of M1, M3, and M5 were significantly higher than this. The M5, M3, and M1 specimens sintered at 1400, 1500, and 1600 °C, respectively, were the densest. Thus, at higher sintering temperatures, less MCAS was required for densification presumably because melting-induced loss occurred when excess MCAS was used [25, 26].

XRD analysis

The XRD spectra and corresponding full width at half maximum (FWHM) of the samples prepared with different MCAS contents and sintered at different temperatures are shown in Fig. 4. Fig. 4(a) shows the XRD spectra of the specimens sintered at 1500 °C. No

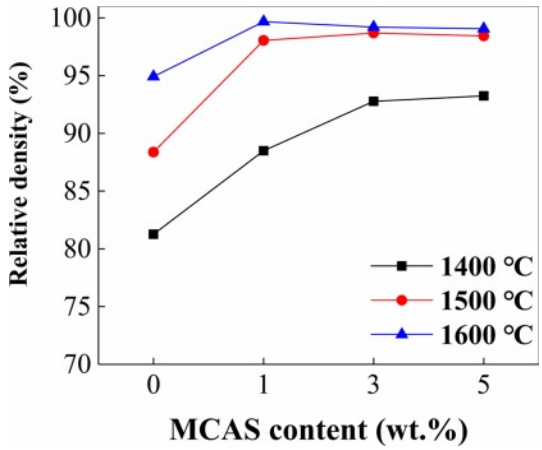

Fig. 3. Relative density of Al_2O_3 plotted as functions of MCAS content for different sintering temperatures.

MCAS peak was observed in the spectra of these samples because MCAS is an amorphous substance unsuitable for XRD analysis. Fig. 4(b) presents the FWHM for the main peak of the (116) plane for M0 sintered at various temperatures. According to the Scherrer equation, FWHM is related to crystallinity [27]. Clearly, FWHM decreased with increasing sintering temperature, indicating that grain growth had occurred. Fig. 4(c) shows the FWHM for the (116) peak at each sintering temperature for the samples prepared with different MCAS contents. Although increasing the MCAS content did not result in a clear FWHM trend for the Al_2O_3 samples sintered at 1400 °C, the FWHM of the samples sintered at 1500 and 1600 °C decreased somewhat and considerably, respectively. Considering both the results shown in Fig. 4(c) and the shrinkage behavior shown in Fig. 2 suggests that grain growth did not occur at 1400 °C because shrinkage was incomplete. By contrast, at 1500 and 1600 °C, it appears that the addition of MCAS accelerated Al_2O_3-particle binding through liquid-phase formation and caused grain growth.

Microstructural analysis

Fig. 5 shows polished cross-sectional images of sintered Al_2O_3. Fig. 5(a)-(c) presents microstructural

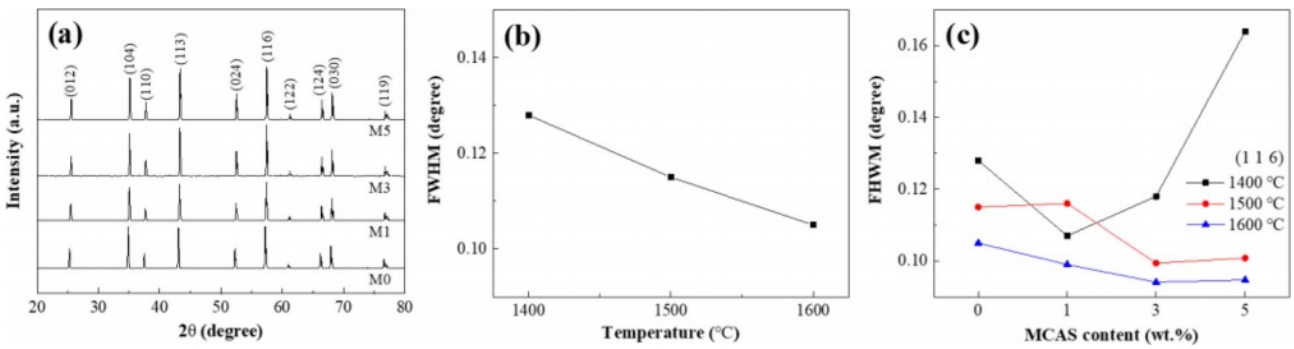

Fig. 4. (a) XRD spectra for M0, M1, M3, and M5 sintered at 1500 °C; FWHM for (116)-plane peak plotted as functions of (b) sintering temperature and (c) MCAS content.

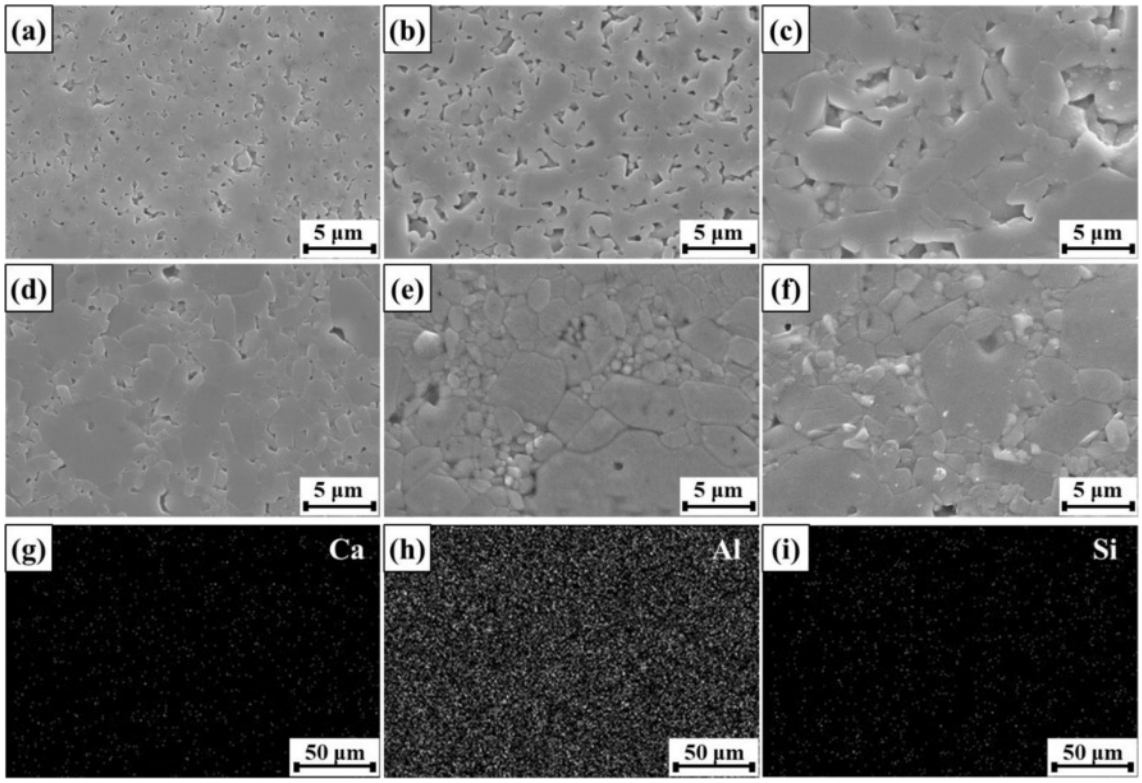

Fig. 5. Polished cross-sectional SEM images of M0 sintered at (a) 1400, (b) 1500, and (c) 1600 °C; polished cross-sectional SEM images of (d) M1, (e) M3, and (f) M5 sintered at 1500 °C; EDS maps of (g) Ca, (h) Al, and (i) Si for M5 sintered at 1500 °C.

images of M0 sintered at 1400, 1500, and 1600 °C, respectively. Like the raw material, the specimen sintered at 1400 °C exhibited particles several hundred nanometers in diameter. From the dilatometry results shown in Fig. 2, densification was incomplete at 1400 °C; thus, grain growth was not observed. In contrast, densification was complete above 1500 °C; thus, grain growth occurred, and grain size increased with increasing sintering temperature. The microstructures of M1, M3, and M5 sintered at 1500 °C are shown in Fig. 5(d), (e), and (f), respectively. Clearly, grain size increased with increasing MCAS content. MCAS has a low melting point (1050 °C), and its glass-transition temperature is approximately 670 °C [24]. Therefore, MCAS densified the Al_2O_3 particles below the M0 densification temperature and accelerated particle growth by facilitating the formation of necks between Al_2O_3 particles. The change in particle size observed through SEM was also consistent with the FWHM trend shown in Fig. 3. These results show that particle size can be controlled by adjusting both the sintering temperature and the MCAS content. Additionally, surface EDS analysis confirmed that individual MCAS elements were not segregated and were evenly distributed throughout the specimens, as shown in Fig. 5(g)-(i).

Hardness test

Fig. 6 shows the hardness of the Al_2O_3 bodies prepared with different MCAS contents and sintered at

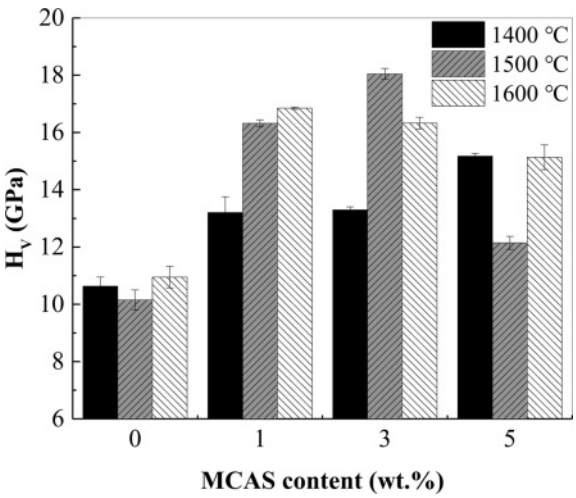

Fig. 6. Hardness of Al_2O_3 bodies prepared with different MCAS contents and sintered at different temperatures.

different temperatures. The measured hardness values showed a trend like that of the sintered-body densities, as shown in Fig. 4. For the specimen sintered at 1400 °C, the hardness was extremely low owing to the low sintering density, indicating low bonding strength between the Al_2O_3 particles. However, with increasing MCAS content, the bonding strength between the Al_2O_3 particles increased; therefore, hardness increased. For the specimens sintered at 1500 and 1600 °C, the increase in hardness was substantial. However, M5

sintered at these temperatures exhibited excessive grain growth, which decreased hardness [28]; therefore, the highest hardness of 18 GPa was achieved by M3 sintered at 1500 ºC.

Conclusions

This study investigated the effects of the sintering temperature and MCAS-additive content on Al_2O_3 sintering behavior. The main results are summarized as follows:

(1) Al_2O_3 sintering behavior was analyzed using a dilatometer, and the results showed that the addition of MCAS accelerated densification, which was completed below 1600 ºC.

(2) A high relative density of 98% was achieved by adding MCAS at a relatively low sintering temperature of 1500 ºC.

(3) XRD and SEM analyses confirmed that the Al_2O_3 microstructure could be tailored by tuning both the sintering temperature and MCAS content.

These results will elucidate the conditions required to prepare high-density Al_2O_3 for practical applications.

Acknowledgements

This work was supported by the Korea Institute of Ceramics Engineering and Technology and the Ministry of Trade, Industry, and Energy (MOTIE), under Grant 20003891.

References

1. M.P. Harmer and R.J. Brook, J. Mater. Sci. 15 (1980) 3017-3024.
2. M.P. Harmer and R.J. Brook, J. Br. Ceram. Soc. 5 (1981) 147-148.
3. C. Nivot and F. Valdivieso, Ceram. Int. 34 (2008) 1595-1602.
4. K. Liu, Y. Shi, W. He, C. Li, Q. Wei, and J. Liu, Int. J. Adv. Manuf. Technol. 67 (2013) 2511-2519.
5. G. Maizza, S. Grasso, and Y. Sakka, J. Asian Ceram. Soc. 2[3] (2014) 215-222.
6. P. Guyot, G. Antou, N. Pradeilles, A. Weibel, M. Vandenhende, G. Chevallier, A. Peigney, C. Estournès, and A. Maître, Scr. Mater. 84-85 (2014) 35-38.
7. A. Moradkhani, H. Baharvandi, and A. Naserifar, J. Korean Ceram. Soc. 56 (2019) 256-268.
8. J. Song, Y. Liu, C. Pang, J. Zhang, L. Chen, X. Zhang, S. Guo, X. Wang, R. Wang, and A. Chen, J. Ceram. Process. Res. 19 (2018) 142-145.
9. K. Shigeno, H. Katsumura, H. Kagata, H. Asano, and O. Inoue, Ferroelectrics, 356 (2007) 189-196.
10. H. Unno, Y. Sato, S. Toh, N. Yoshinaga, and S. Matsumura, J. Electron Microsc. 59 (2010) S107-S115.
11. T.H. Byeon, H.S. Park, H. H. Shin, S. O. Yoon, and C.Y. Oh,, J. Korean Ceram. Soc. 47 (2010) 325-328.
12. I.J. Induja, P. Abhilash, S. Arun, K.P. Surendran, and M.T. Sebastian, Ceram. Int. 41 (2015) 13572-13581.
13. X. Luo, L. Ren, Y. Hu, Y. Xia, M. Xin, C. Zhang, and H. Zhou, Ceram. Int. 44 (2018) 6354-6361.
14. B.R. Cho, J.J. Lee, and S.K. Kang, J. Ceram. Process. Res. 10 (2009) 121-123.
15. W.R. Rao and I.B. Cutler, J. Am. Ceram. Soc. 56 (1973) 588-593.
16. J. Zhao and M.P. Harmer, J. Am. Ceram. Soc. 70 (1987) 860-866.
17. Z. Harun, N.F. Ismail, and N.A. Badarulzaman, Adv. Mat. Res. 488-489 (2012) 335-339.
18. S. Lei, H. Fan, and W. Chen, J. Alloys. Compd. 632 (2015) 78-86.
19. C.M. Cheng, C.F. Yang, S. H. Lo, and T.Y. Tseng, J. Eur. Ceram. Soc. 20 (2000) 1061-1067.
20. H.J. Lee, S.W. Kim, and S.S. Ryu, Int. J. Refract. Met. Hard Mater. 53 (2015) 46-50.
21. H.J. Lee, W.S. Cho, H.J, Kim, H.T. Kim, and S.S. Ryu, J. Korean Ceram. Soc. 54 (2017) 43-48.
22. O. Kaygili, F. Yakuphanoglu, and C. Tatar, J. Ceram. Process. Res. 17 (2016) 881-884.
23. H.J. Lee, W.S. Cho, H.J. Kim, W. Pan, M. Shahid, and S.S. Ryu, Electron. Mater. Lett. 12 (2016) 732-737.
24. K. Agersted and T. Balic-Zunic, Int. J. Appl. Ceram. Technol. 15 (2018) 255-266.
25. K. Chen, Y. Pu, N. Xu, and X. Luo, Electron. Mater. Lett. 23 (2012) 1599-1603.
26. S. Qi, H. Cheng, K. Yang, B. Song, S. Sun, and Y. Zhang, J. Mater. Sci.: Mater. Electron. 30 (2019) 6411-6418.
27. G.K. Williamson and W.H. Hall, Acta Metall. 1 (1953) 22-31.
28. G. Mata-Osoro, J.S. Moya, and C. Pecharroman, J. Eur. Ceram. Soc. 32 (2012) 2925-2933.